

Electron transport in a toroidal carbon nanotube device

C.P. Liu^a, Z.X. Guo^a, J.W. Ding^{a,b,*}, X.H. Yan^{a,c}

^a*Department of Physics, Xiangtan University, Xiangtan 411105, Hunan, China*

^b*National Laboratory of Solid State Macrostructures, Nanjing University, Nanjing 210093, China*

^c*College of Science, Nanjing University of Aeronautics and Astronautics, Nanjing 210016, China*

Received 11 April 2005; accepted 3 May 2005

Abstract

Taking the curvature and disorder into account, the electron transport in a carbon molecular device consisting of a toroidal carbon nanotube connected with two semi-infinite metallic carbon nanotubes, has been investigated by using the tight-binding Green's function method and the Landauer–Büttiker formula. It is shown that the current through the device can be modulated by the disorder in the molecular device and/or the torus-tube distance. The negative differential conductance is obtained at relatively large bias, while the current has little increase for small voltages. The results are in good agreement with the experimental observation.

© 2005 Elsevier B.V. All rights reserved.

PACS: 73.61.wp; 73.63.–b

Keywords: Toroidal carbon nanotube; Tight-binding Green's function; Negative differential conductance

1. Introduction

Carbon atoms can form many kinds of structures, such as diamond, graphite, C₆₀, carbon nanotube (CNT) [1]. A single-wall CNT could be regarded as a rolled-up graphite sheet in cylindrical form. It is found that such a CNT can be bent within the crystalline nanotube rope [2] and form a toroidal carbon nanotube (TCNT) [3,4]. Such

TCNTs were firstly observed by Liu et al. [3] and can be synthesized in the gross [4]. These closed-ring structures may be used as building blocks of small electromagnetic devices and their structures and electronic properties are of primary interest for such applications [5–14]. Theoretically, for example, Hod et al. [11] studied the structure and stability of TCNTs, and many metastable structures were obtained. Liu et al. [6] calculated the electronic and magnetic properties of TCNTs, showing that a type of TCNTs are paramagnetic at any radius and another type of TCNTs may exhibit giant paramagnetic moments only at selected radii. Experimentally, the characteristic

*Corresponding author. Tel.: +86 7328293798;
fax: +86 7328229468.

E-mail addresses: cpliu@xtu.edu.cn (C.P. Liu),
jwding@xtu.edu.cn (J.W. Ding).

of weak one-dimensional localization is clearly observed from the magnetoresistance measurements of the TCNTs at low temperature [12]. Moreover, Watanabe et al. [13] constructed a dual-probe scanning tunneling microscope (STM) with two multi-walls CNT probes and measured the current–voltage curves of a single TCNT as a transistor. The results illustrate exciting possibility of nanometer-scale electronic circuits composed of TCNT devices.

When bending a finite length CNT to a TCNT, on the other hand, the curvatures may result in the large variations of the bond length between two nearest-neighbor carbon atoms and thus has an important effect on the electronic structures of the TCNTs. In the procedure of both the preparation and the measurement, also, the TCNTs may be subjected to various mechanical deformations or can adsorb some gas molecules from its exposed environment. So, it is expected that the transport behavior in the TCNTs will be influenced by the disorders induced by the deformation and the adsorbates etc. As a result, the effects of curvature and disorder should be taken into account to explore the transport properties of the TCNT-based nanostructure.

In this paper, a model of the CNT–TCNT–CNT molecular device is built, in which the curvature and disorder effects are taken into account. The electron transport through the device is calculated by using the tight-binding Green's function method and the Landauer–Büttiker formula. It is shown that the disorder strength and the TCNT–CNT distance D (shown in Fig. 1) plays an important role in determining the current–voltage characteristic. The negative differential conductance is obtained at relatively large bias, while the current has little increase for small voltages. The results are in good agreement with the experimental observation.

2. Geometric structure of a CNT–TCNT–CNT molecular device

A TCNT can be formed from a finite length (n,m) nanotube (containing p primitive cells), curled up onto a torus. Such a torus will be

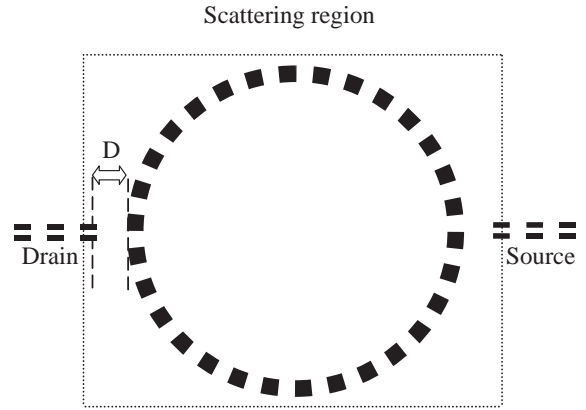


Fig. 1. The schematic representation of a (6,6,30) TCNT connected with two metallic semi-infinite (6,0) CNTs. The dashed-line frame encloses the scattering region.

referred as (n,m,p) TCNT [10]. Here we consider a (6,6,30) TCNT connected by two metallic semi-infinite (6,0) CNTs on the left- and right-hand sides as two leads, as shown in Fig. 1. Such a hybrid system is referred as (6,0)–(6,6,30)–(6,0) molecular device. Each lead is separated from the TCNT by distance D , taken as a parameter in our calculation. The TCNT and the first unit cells of the two CNTs (nearest to TCNT) constitute the scattering region [15].

3. Model Hamiltonian and Green's function method

The TCNT can be viewed as a molecule or a cluster but has a much larger number of atoms relatively. Due to the destruction of translation symmetry in the system, we treat the Hamiltonian entirely in real space within a single π -orbital tight-binding approximation [9,10], given by [16]

$$H = \sum_i \varepsilon_i^0 c_i^\dagger c_i + \sum_{ij} t_{ij} c_i^\dagger c_j, \quad (1)$$

where ε_i^0 is the on-site potential, t_{ij} the hopping parameter between grid points i and j , and $\{c_i^\dagger, c_i\}$ are the creation and annihilation operators at site i . In our model, the two semi-infinite CNT leads are assumed to be perfect, in which ε_i^0 is fixed to Fermi energy E_F , and $t_{ij} = -3.00$ eV [9]. This enables us to focus on the transport characteristic

of the TCNT scattering region. Due to the curvature-induced changes in bond-length d_{ij} , the hopping parameter t_{ij} for the scattering region is multiplied by a modified factor $f(d_{ij})$ [17]. To model the disorder in the sample, the on-site potential is taken to be

$$\varepsilon_i^0 \rightarrow \varepsilon_i^0 + \delta\varepsilon_i, \quad (2)$$

where $\delta\varepsilon_i$ is randomly chosen from the interval $[-W, W]$. W is the disorder strength.

When an external voltage is applied on the two leads, the system is driven out of equilibrium in its bid to equilibrate with both leads, causing a current flow [18]. For simplification, we assume a linear drop in the applied voltages [16]. The effect of electric field is then incorporated into the on-site energies [19]. The retarded Green's function for the scattering region is given by [20]

$$G(E) = [E - H_C - \Sigma_L - \Sigma_R]^{-1}, \quad (3)$$

where H_C is the Hamiltonian of the scattering region. The self-energy matrices $\Sigma_{L,R}$ due to the semi-infinite leads can be viewed as effective Hamiltonians, which allows us to replace an infinite open system with a finite one [20]. Following Nardelli et al. [21], the self-energy is calculated by using an iterative procedure. The electron transmission probability across the scattering region at energy E can be obtained by [16]

$$T(E) = \text{Tr}[\Gamma_L G \Gamma_R G^+], \quad (4)$$

where G^+ is the corresponding advanced Green's-function matrix. The level broadenings $\Gamma_{L,R}$ describe the coupling of the scattering region to the left and right leads, given by

$$\Gamma_{L,R} = i[\Sigma_{L,R} - \Sigma_{L,R}^+]. \quad (5)$$

The current through the device is then calculated by using the Landauer–Buttiker formula,

$$I = \frac{2e}{h} \int dE T(E) [f_L - f_R], \quad (6)$$

where $f_{L,R}$ is the Fermi functions for the left lead (drain electrode) and right lead (source electrode), respectively. The chemical potentials for the two leads can be written as $\mu_{L,R} = E_F \mp eV/2$, with V being the external voltage applied between the two electrodes.

4. Calculations and discussions

As a typical example, the (6,0)–(6,6,30)–(6,0) molecular device has been studied to explore its dependence of electron transport on the disorder and the CNT–TCNT distance D .

In Fig. 2, we first calculate the transmission spectrum of the molecular device with $D = 1.5$ Å in the absence of both disorder and external voltage ($W = 0$ and $V = 0$). For a comparison, the calculated transmission spectra of the perfect (6,0) and (6,6) CNTs are also shown. As expected, the two perfect metallic tubes exhibit the step-like features with two units of quantum conductance, consistent with previous prediction. As for the molecular device, the overall conductance is depressed to be under those of the (6,0) and (6,6) CNTs. Interestingly, the resonant structures are observed from Fig. 2 in the transmission spectrum of the molecular device, showing the similar characteristic of the C60 molecular electronic device [15], which may be due to the quantum confinement of the finite size TCNT. Also, there appear a few conductance gaps and a largest conductance gap is formed at E_F , contrary with the results of a metallic TCNT [14], which can be attributed to the scattering in the contact as well as the heavy curvature effects. This means that the curvature and contact effects should be fully

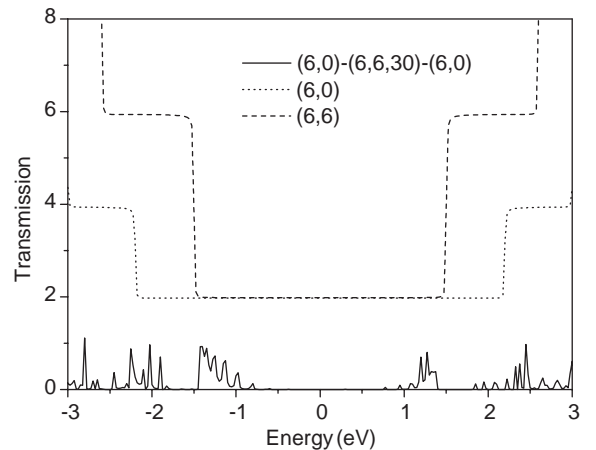


Fig. 2. The transmission spectrum of the (6,0)–(6,6,30)–(6,0) molecular device. Also shown are the calculated transmission spectra for the perfect (6,0) and (6,6) nanotubes.

considered to study the transport properties of such a TCNT-based nanodevice.

Fig. 3 shows the calculated I - V curves of the molecular device with $D = 1.5 \text{ \AA}$ for varying disorder strength W at room temperature ($T = 300 \text{ K}$). Under small applied voltages ($V < 0.6 \text{ V}$), the current seems to be almost independent of disorder strength and has little increase with the increasing bias, similar to that of carbon nanotube ropes measured by Collins et al. [22]. This may be ascribed to few conduction channels existing in the energy window $[-0.4, 0.4 \text{ eV}]$ even for varying W . For large applied voltages ($V > 1 \text{ V}$), the current tends to increase obviously with increasing voltage except for the case of $W = 0$, and its magnitude is much larger compared with that for small applied voltages ($V < 0.6 \text{ V}$), showing on-off characteristic. This indicates that one may exploit an electronic switch based on this nanodevice. Interestingly, the negative differential conductance (NDC) appears in the I - V curves, which has been observed in the TCNT-based transistor [13]. The NDC can be ascribed to the tunneling through the device and has a wide range potential device application [23]. At large applied bias, additionally, it can be found that the current becomes generally large with W increasing. This may be attributed to the fact that the increase of W in a certain range may result in the increase of the total density of states in the energy region $[-2, 2 \text{ eV}]$ [24]. The conduction

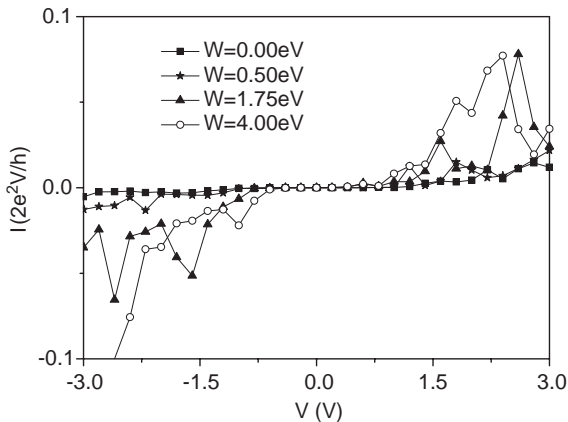


Fig. 3. The calculated I - V curves of the (6,0)-(6,6,30)-(6,0) molecular device for varying disorder strength.

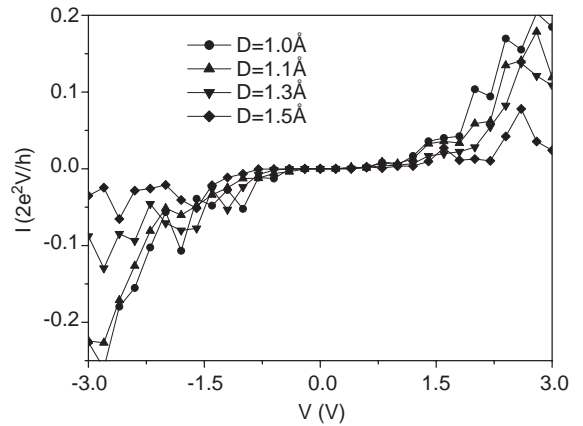


Fig. 4. The calculated I - V curves of the (6,0)-(6,6,30)-(6,0) molecular device for varying distance D . The other parameters are $W = 1.75 \text{ eV}$ and $T = 300 \text{ K}$.

channels introduced into this energy region have the additional contribution to the current.

In the practical STM experiments, the distance D of the STM probes from the measured TCNT can be varied. The coupling strength between the TCNT and leads are then changed, decreasing with D increasing. To explore the coupling effects, we further calculate in Fig. 4 the I - V curves of the molecular device for varying D . At larger bias voltages ($V > 1 \text{ V}$), the current generally increases with D decreasing, while it is almost independent of the distance D at small applied voltages ($V < 0.4 \text{ V}$). This may be due to the fact that the reduction of D can increase the coupling between the TCNT and leads, leading to more effective conduction channels in the case of large bias. Therefore, one could change the transport properties of such molecular devices through varying the distance D and thus manipulate its performance at will.

5. Conclusions

We have calculated the phase-coherent transmission through TCNT connected with two perfect CNTs under external voltages by using the tight-binding Green's function method and the Landauer-Büttiker formula. The dependence of transport properties on the disorder strength and

the CNT–TCNT distance was discussed. The negative differential conductance is obtained at relatively large bias, while the current has little increase for small voltages. The obtained results can provide a qualitative understanding of the transport properties of such molecular devices, and give a foundation for the design and application of the molecular devices.

Acknowledgments

This work is supported by the National Natural Science Foundation of China under Grant No 10447129, the Natural Science Foundation of Hu'nan Province, China under Grant No 04JJ3041, and partially by the Research Foundation of Education Bureau of Hu'nan Province under Grant No 03B039.

References

- [1] S. Iijima, *Nature* (London) 354 (1991) 56.
- [2] A. Thess, et al., *Science* 273 (1996) 438.
- [3] J. Liu, H. Dai, J.H. Hafner, D.T. Colbert, R.E. Smalley, S.J. Tans, C. Dekker, *Nature* (London) 385 (1997) 780.
- [4] M. Sano, A. Kamino, J. Okamura, S. Shinkai, *Science* 293 (2001) 1299.
- [5] M.F. Lin, D.S. Chuu, *Phys. Rev. B* 57 (1998) 6731.
- [6] L. Liu, G.-Y. Guo, C.S. Jayanthi, S.Y. Wu, *Phys. Rev. Lett.* 88 (2002) 217206.
- [7] D.H. Oh, J.M. Park, K.S. Kim, *Phys. Rev. B* 62 (2000) 1600.
- [8] H.K. Zhao, *Phys. Lett. A* 317 (2003) 329.
- [9] A. Latge, C.G. Rocha, L.A.L. Wanderley, M. Pacheco, P. Orellana, Z. Barticevic, *Phys. Rev. B* 67 (2003) 155413.
- [10] S. Latil, S. Roche, A. Rubio, *Phys. Rev. B* 67 (2003) 165420.
- [11] O. Hod, E. Rabani, *Phys. Rev. B* 67 (2003) 195408.
- [12] H.R. Shea, R. Martel, Ph. Avouris, *Phys. Rev. Lett.* 84 (2000) 4441.
- [13] H. Watanabe, C. Manabe, T. Shigematsu, M. Shimizu, *Appl. Phys. Lett.* 78 (2001) 2928.
- [14] Y.Y. Chou, G.-Y. Guo, Lei Liu, C.S. Jayanthi, S.Y. Wu, *J. Appl. Phys.* 96 (2004) 2249.
- [15] R. Gutierrez, G. Fagas, G. Cuniberti, F. Grossmann, R. Schmidt, K. Richter, *Phys. Rev. B* 65 (2002) 113410.
- [16] M.P. Anantram, T.R. Govindan, *Phys. Rev. B* 58 (1998) 4882.
- [17] J.W. Ding, X.H. Yan, J.X. Cao, D.L. Wang, Y. Tang, Q.B. Yang, *J. Phys: Condens. Matter* 15 (2003) L439.
- [18] G.C. Liang, A.W. Ghosh, M. Paulsson, S. Datta, *Phys. Rev. B* 69 (2004) 115302.
- [19] Y. Kim, K. Chang, *Phys. Rev. B* 64 (2001) 153404.
- [20] S. Datta, *Electronic Transport in Mesoscopic Systems*, Cambridge University Press, New York, 1995.
- [21] M.B. Nardelli, *Phys. Rev. B* 60 (1999) 7828.
- [22] P.G. Collins, A. Zettl, H. Bando, A. Thess, R.E. Smalley, *Science* 278 (1997) 100.
- [23] F. Leonard, J. Tersoff, *Phys. Rev. Lett.* 85 (2000) 4767.
- [24] S. Roche, R. Saito, *Phys. Rev. B* 59 (1999) 5242.